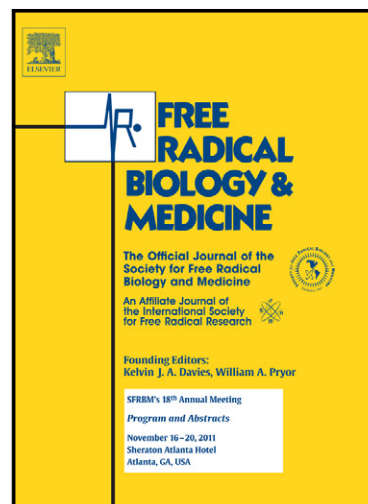


Author's Accepted Manuscript

8-Oxoguanine DNA glycosylase-1-mediated DNA repair is associated with Rho-GTPase activation and smooth muscle α -actin polymerization

Jixian Luo, Koa Hosoki, Attila Bacsi, Zsolt Radak, Muralidhar L. Hegde, Sanjiv Sur, Tapas K Hazra, Allan R. Brasier, Xueqing Ba, Istvan Boldogh



www.elsevier.com/locate/freerad-biomed

PII: S0891-5849(14)00147-6
DOI: <http://dx.doi.org/10.1016/j.freeradbiomed.2014.03.030>
Reference: FRB11961

To appear in: *Free Radical Biology and Medicine*

Received date: 4 January 2014
Revised date: 12 March 2014
Accepted date: 19 March 2014

Cite this article as: Jixian Luo, Koa Hosoki, Attila Bacsi, Zsolt Radak, Muralidhar L. Hegde, Sanjiv Sur, Tapas K Hazra, Allan R. Brasier, Xueqing Ba, Istvan Boldogh, 8-Oxoguanine DNA glycosylase-1-mediated DNA repair is associated with Rho-GTPase activation and smooth muscle α -actin polymerization, *Free Radical Biology and Medicine*, <http://dx.doi.org/10.1016/j.freeradbiomed.2014.03.030>

This is a PDF file of an unedited manuscript that has been accepted for publication. As a service to our customers we are providing this early version of the manuscript. The manuscript will undergo copyediting, typesetting, and review of the resulting galley proof before it is published in its final citable form. Please note that during the production process errors may be discovered which could affect the content, and all legal disclaimers that apply to the journal pertain.

**8-Oxoguanine DNA glycosylase-1-mediated DNA repair is associated with
Rho-GTPase activation and smooth muscle α -actin polymerization**

Jixian Luo^{a,1}, Koa Hosoki^{c,2}, Attila Bacsi^{a,3}, Zsolt Radak^{a,4}, Muralidhar L. Hegde^{b,5}
Sanjiv Sur^{c,d}, Tapas K Hazra^{c,d}, Allan R. Brasier^{b,d}, Xueqing Ba^{a,6}, Istvan Boldogh^{a,d*}

^aDepartments of Microbiology and Immunology, ^bBiochemistry and Molecular
Biology, ^cInternal Medicine, ^dSealy Center for Molecular Medicine, University of
Texas Medical Branch at Galveston, Galveston, TX 77555, USA

Permanent address:

¹School of Life Science, Shanxi University, Taiyuan, China

²Institute for Clinical Research, Mie National Hospital, Mie, Japan

³Department of Immunology, Medical and Health Science Center, University of
Debrecen, Debrecen, Hungary

⁴Research Institute of Sport Science, Semmelweis University, Budapest, Hungary

⁵Radiation Oncology, Houston Methodist Research Institute, Houston TX, USA

⁶Key Laboratory of Molecular Epigenetics, Institute of Genetics and Cytology,
Northeast Normal University, Changchun, China

***Corresponding author:**

Istvan Boldogh, DM&B, PhD
Department of Microbiology and Immunology
University of Texas Medical Branch at Galveston
301 University Blvd, Galveston, Texas 77555-1070
Telephone: 409-772-9414, Fax: 409-747-6869
Email: (sboldogh@utmb.edu)

Abstract

Reactive oxygen species (ROS) are activators of cell signaling and modify cellular molecules, including DNA. 8-oxo-7,8-dihydro-guanine (8-oxoG) is one of the prominent lesions in oxidatively damaged DNA, whose accumulation is causally linked to various diseases and aging processes, while its etiological relevance is unclear. 8-oxoG is repaired by the 8-oxoguanine DNA glycosylase-1 (OGG1)-initiated DNA base excision repair pathway (BER). OGG1 binds free 8-oxoG and this complex functions as an activator of Ras family GTPases. Here we examined whether OGG1-initiated BER is associated with the activation of Rho-GTPase and mediate changes in the cytoskeleton. To test this possibility, we induced OGG1-initiated BER in cultured cells and mouse lungs, and used molecular approaches such as active Rho pull-down assays, siRNA ablation of gene expression, immune blotting and microscopic imaging. We found that OGG1 physically interacts with Rho-GTPase, and in the presence of 8-oxoG base, increases Rho-GTP levels in cultured cells and lungs, which mediated smooth muscle α -actin (α -SMA) polymerization into stress fiber and increased the level of α -SMA in insoluble cellular/tissue fractions. These changes were absent in cells lacking OGG1. These unexpected data and those showing that 8-oxoG repair is a lifetime process suggest that via Rho-GTPase, OGG1 could be involved in the cytoskeletal changes and organ remodeling observed in various chronic diseases.

Key words: ROS, OGG1, base excision repair, Rho-GTP cytoskeleton

Highlights

► 8-oxoguanine DNA glycosylase-1 (OGG1) excises 8-oxoguanine (8-oxoG) as a base from DNA. ► OGG1 physically interacts with RhoA. ► OGG1 in the presence of 8-oxoG activates RhoA GTPase. ► Active RhoA links OGG1-BER to α -SMA polymerization into stress fibers.

Accepted manuscript

Abbreviations:

8-oxoG: 8-Oxo-7, 8-dihydroguanine

8-oxodG: 8-oxo-7,8-dihydro-2'-deoxyguanosine

α -SMA: alpha smooth muscle actin

Ab: antibody

BER: base excision repair

FU: fluorescence unit

FapyG: 2,6-diamino-4-hydroxy-5-formamidopyrimidine

GEF: guanine nucleotide exchange factor

GST: Glutathione-S-Transferase

^{Mant}GTP: GTP (2'-(or-3')-*O*-(*N*-methylantraniloyl) guanosine 5'-triphosphate

^{Mant}GDP: GDP (2'-(or-3')-*O*-(*N*-methylantraniloyl) guanosine 5'-diphosphate

OGG1: 8-oxoguanine DNA glycosylase-1

Accepted manuscript

1. Introduction

Oxidative stress is generated by multiple exogenous agents and endogenous sources in mammalian cells. The resulting reactive oxygen species (ROS) cause damage to cellular molecules, including DNA [1]. In the DNA guanine is a primary ROS target because it has the lowest reduction potential among nucleic acid bases [2]; 7,8-dihydro-8-oxoguanine (8-oxoG) is thus one of the most abundant base lesions. Due to its potential to pair with adenine, 8-oxoG is also one of the most mutagenic DNA lesions among over 20 identified oxidative modifications to guanine [3, 4]. Accumulation of 8-oxoG in DNA has been linked to various inflammatory diseases, as well as aging processes [5]. The oxidatively damaged bases are preferentially repaired by the base excision repair (BER) pathway [6, 7], which utilizes glycosylases to excise the lesion via cleaving its N-glycosidic bond, followed by endonucleolytic cleavage and subsequent gap-filling [6, 8].

8-oxoguanine DNA glycosylase (OGG1) is the key enzyme in removing 8-oxoG and 2,6-diamino-4-hydroxy-5-formamidopyrimidine (FapyG) from DNA equal specificity and kinetics during BER to prevent mutations and maintain genomic integrity [6, 9, 10]. Surprisingly, *Ogg1* knockout (KO) mice have no particular phenotype; their life span is unaltered, showing only a moderate predisposition to tumorigenesis, despite increased genomic 8-oxoG levels [11-13]. A lack of OGG1 activity in KO mice resulted in increased resistance to inflammation [14], changes in whole-body energy homeostasis, increased susceptibility to obesity, and metabolic dysfunction [15]. These results suggest additional, not yet defined function(s) of OGG1 protein and/or its repair product, 8-oxoG. In support of this hypothesis, accumulating data suggest that OGG1 may play roles in multiple cellular processes. For example, it has been shown that OGG1 co-localizes with centrioles (microtubule organizing centers), microtubule networks, and mitotic chromosomes [16, 17]. It has also been shown that OGG1-generated free 8-oxoG base binds to OGG1 and increases its β -lyase activity, mediating product-assisted catalysis in an enzyme-catalyzed reaction [18]. Our recent studies also showed that 8-oxoG binds cytoplasmic OGG1, and the OGG1•8-oxoG complex acts as a guanine nucleotide exchange factor (GEF)

catalyzing the exchange of GDP with GTP to promote activation of Ras and Rac1 small GTPases [19-21].

In response to DNA damage, or in DNA damage-induced senescent cells, reorganization of the cytoskeleton, actin filaments (stress fibers) and filopodia has been observed [22], although the molecular events directly responsible for these cytoskeletal morphological changes are not yet well-defined. Among the small GTPase family members, activation of the Ras homology (Rho) proteins RhoA, RhoB and RhoC has been shown to regulate many aspects of intracellular actin dynamics, including stress fiber formation [23]. Taking into account that OGG1 functions as a GEF when complexed with 8-oxoG [19-21], we hypothesized that OGG1-BER is associated with Rho activation and transient morphological changes in ROS-exposed cells. Here we show that OGG1-initiated repair of oxidative DNA damage was followed by an increase in Rho-GTP levels and stress fiber formation in cultured cells and lung tissues. Thus our studies establish a link between repair of oxidatively altered guanine and changes in cellular architecture, placing OGG1 at the center of a complex signaling network.

Accepted

2. Materials and Methods

Materials

8-oxoG (8-Oxo-7, 8-dihydroguanine, cat #89290) was from Cayman Chemical Company (Michigan, USA); 2,6-diamino-4-hydroxy-5-formamidopyrimidine (Fapy G) was a kind gift of Dr. Miral Dizdaroglu (National Institute of Standards and Technology, Gaithersburg, MD); glucose oxidase from *Aspergillus niger* (GOx, cat # G7141-10KU), FITC-conjugated phalloidin (cat # P5282-.1MG), Triethanolamine (TEA, cat # 90279-100ML), N-TERTM Nanoparticle siRNA Transfection System (cat # N2913) were from Sigma-Aldrich (St. Louis, USA); rabbit polyclonal antibody (Ab) to alpha smooth muscle actin (anti- α -SMA, cat # ab5694) was from Abcam (Cambridge, USA); monoclonal Abs to GAPDH (cat # 2118S) and α -tubulin (cat # 3873S) were from Cell Signaling Technology, Inc. (Danvers, USA); active Rho pull-down and detection kit (cat # 16116Y) was from Thermo Scientific Pierce Biotechnology (Rockford, USA); OGG1 rabbit monoclonal Ab (cat # 5104-1) was from the Abcam subsidiary Epitomics (Burlingame, USA). siGENOME SMARTpool for human OGG1 (cat # M-005147-03) was from Dharmacon Thermo Scientific (Pittsburgh, USA). Rho activator (calpeptin, cat # CN01) and Rho inhibitor (C3 transferase, cat # CT04) were from Cytoskeleton (Denver, USA); His-tagged RhoA protein (cat # NBP1-50933) was from Novus Biologicals (Littleton, USA) and OGG1 protein was a kind gift from Dr. Hazra (Department of Biochemistry & Molecular Biology, UTMB, USA). (2'-(or-3')-O-(N-methylanthraniloyl) guanosine 5'-triphosphate (Mant)-GTP (^{Mant}GTP) and ^{Mant}GDP were from Cytoskeleton (Denver, USA).

Cell Culture

Human diploid fibroblast (MRC5) and mouse embryonic fibroblast (MEF) cells were maintained in Earle's minimum essential medium and DMEM/F-12 (Ham) supplemented with 10% fetal bovine serum, glutamine, penicillin, and streptomycin; cells were grown at 37 °C in 5% CO₂, starved in 0.5% FBS medium for 24 h, and

starved in FBS free medium for 16 h before Rho activation. 8-oxoG (10 μ M) or GOx (100 ng/ml) was added to cells in serum-free media, and cell extracts were made at the indicated times after 8-oxoG or GOx addition.

Animals

Animal experiments were performed according to the National Institutes of Health Guidelines for Use of Experimental Animals and approved by the University of Texas Animal Care and Use Committee (Protocol number: 0807044A). Eight-week-old female BALB/c mice (the Jackson Laboratory, Bar Harbor Maine) were challenged intranasally with 1 μ M 8-oxoG (60 μ l) or equal volume of vehicle, sacrificed, and lungs were excised [24]. In other experiments, mice were directly sacrificed without treatment.

Histology and immunohistochemistry

For immunohistochemistry staining of α -SMA or F-actin, mice were challenged with 1 μ M 8-oxoG (in 60 μ l PBS), and sacrificed after 30 min. Mouse lungs were fixed, sectioned (4 μ m) and stained with α -SMA Ab and/or FITC-phalloidin. Cells on chambers slides were challenged with the OGG1-initiated BER byproduct 8-oxoG for 20 min and after treatment fixed with 4% paraformaldehyde for 20 min at room temperature, then washed twice with wash buffer (0.05% Tween 20 in PBS) and permeabilized with 0.1% Triton X-100 for 3 min. After washing, blocking solution (1% BSA in 0.05% Tween 20 PBS) was added for 30 min. Mouse anti-rabbit- α -SMA monoclonal Ab and FITC-phalloidin were diluted in the blocking solution. After 1 h incubation with the primary Ab (1:300) followed by three washes with washing buffer, the secondary Ab (goat anti-mouse, FITC-conjugated, dilution 1:500) was added for 30-60 min. Cells were washed with 0.05% Tween 20 in PBS 3-times, dried and mounted in antifade reagent (cat # S3023 from Dako North America, Carpinteria, CA). Stress fibers were visualized under a microscope using FITC-conjugated phalloidin (50 μ g/ml) per the manufacturer's protocol, at 600 \times magnification. Each image shown was a typical one in the field of

view.

Assessment of active Rho levels

Assessment of Rho-GTP levels in cells was conducted using the active Rho pull-down assay kit as recommended by the manufacturer and described previously [19, 20]. Briefly, cells were challenged with 100 ng/ml GOx or 10 μ M 8-oxoG at 37^o C for the indicated times, lysed in 25 mM Tris-HCl, pH 7.5, 150 mM NaCl, 60 mM MgCl₂, 1% Nonidet P-40, and 5% glycerol, and Rho-GTP in 500 μ g extracts were captured by the GST-Rho-binding domain of Rhotekin immobilized to glutathione resin [25]. After washing with binding buffer, the activated Rho (Rho-GTP) was eluted with Laemmli buffer (0.125M Tris-HCl, 4% SDS, 20% glycerol, 10% 2-mercaptoethanol, pH 6.8) and quantified by Western Blot assay using ImageJ 1.46R.

To assess Rho-GTP levels in the lung lysate, mouse lungs were excised and homogenized in lysis buffer provided by the manufacturer (Thermo Scientific Pierce Biotechnology) containing 10 mM EDTA and 60 mM MgCl₂. 10 μ M 8-oxoG were added to 500 μ g lung extracts and incubated at 37^o C for the indicated times. In other experiments, mouse were challenged intranasally with 1 μ M 8-oxoG (60 μ l) for 30 min, sacrificed and mouse lungs were homogenized. Rho-GTP in 500 μ g lung extracts was captured and quantified by Western Blot analysis.

Protein-protein binding assays

To determine the interactions between OGG1 and Rho, we conducted His-affinity pull-down assays as previously described, with slightly modification [19]. Briefly, Nickel-nitrilotriacetic acid (Ni-NTA)-agarose beads (Qiagen Inc., Valencia, CA) were mixed with His-RhoA protein (6 pmol) in 300 μ l of interaction buffer (50 mM NaH₂PO₄, 300 mM NaCl, 20 mM imidazole, 0.05% Tween 20, pH 7.5). After a 30 min incubation at 4 ^oC, His-RhoA-bound beads were washed 3 times, and equimolar, OGG1 (6 pmol), alone or plus 8-oxoG (6 pmol), was added to the interaction buffer. Samples were incubated for 30 min at 4 ^oC, washed twice with interaction buffer, and

eluted with Laemmli buffer at 100°C for 5 min. The eluents were analyzed on Western blots.

Guanine nucleotide exchange assay

GDP-GTP and GTP-GDP exchange on RhoA were determined by real-time fluorescence spectroscopic analysis [21, 26]. Specifically, RhoA (6 pmol) was loaded with the nucleotide analog ^{Mant}GTP or ^{Mant}GDP in exchange buffer containing 20 mM Tris (pH 7.5), 150 mM NaCl, 1 mM dithiothreitol, 50 µg of bovine serum albumin for 30 min. In the case of GDP-GTP exchange, RhoA-^{Mant}GDP and OGG1 protein (6 pmol) + 8-oxoG base (6 pmol) were mixed with untagged GTP. A similar strategy was used to monitor GTP-GDP exchange. Kinetic changes in the fluorescence of RhoA-^{Mant}GDP or RhoA-^{Mant}GTP were determined using a POLARstar Omega reader (BMG LABTECH, Germany). Curves were fitted using MS Excel. The half-life of RhoA-^{Mant}GDP was determined using POLARstar Omega software.

Preparation of soluble and insoluble cellular fractions

Cells were lysed in Triton X-100 buffer (50 mM Tris, pH 7.5, 1 mM EDTA, 1 mM EGTA, 1 mM Na₃VO₄, 5 mM sodium pyrophosphate, 10 mM sodium glycerophosphate, 1% Triton X-100, 50 mM NaF plus 1% Protease Inhibitor Cocktail) and lysates were assayed for protein concentration using the Bradford reagent and then diluted with 2x Laemmli loading buffer for SDS-PAGE. The pellets from cell lysates (Triton X-100-insoluble α -SMA pool) were sonicated in 2x loading buffer before processing for SDS-PAGE [27]. Equal amounts of protein were then loaded onto 4-20% Tris-glycine gels, and electrophoresed for 90 min at 300 mA constant current. Proteins were blotted onto membranes by electrophoretic transfer at 100 V for 1h at 4 °C and α -SMA levels determined by Western blotting.

Isolation of stress fibers

Cells were cultured for 1 day in 100 mm dishes, and starved in 0.5% FBS-containing medium for 16 h before challenge with 8-oxoG base. Stress fibers were

isolated as previously described, with slightly changes [28]. Briefly, cells were washed in ice-cold PBS and then treated with a low-ionic-strength extraction solution consisting of 2.5 mM TEA (pH 8.2) with protease inhibitor cocktail at 4 °C with gentle agitation for 10-40 min, until the dorsal side of the cell became free-floating. Cells were then treated with extraction buffer I (0.05% NP-40, 1% protease inhibitor cocktail in PBS, pH 7.2) for 5 min. At this stage some cells still had the dorsal side and/or the nucleus, which were then removed by gentle shearing under a phase-contrast microscope with a stream of extraction buffer I. The material still attached to culture dishes was gently washed in extraction buffer II (0.5% Triton X-100, 10% protease inhibitor cocktail in PBS, pH 7.2). The extracted material was scraped off from the dish, suspended in extraction buffer II, and the crude stress fiber isolates were suspended in PBS containing protease inhibitor cocktail, pH 7.4) and centrifuged at 100,000 g for 1 h. The pellet containing highly concentrated stress fibers were sonicated in SDS loading buffer and analyzed by Western blot analysis.

siRNA ablation of gene expression

Cells at 60% confluence were transfected with OGG1 siRNA or control siRNA (at 20 nM, as determined in preliminary studies) using the N-TERTM noparticle siRNA Transfection System. After 24h, cells were re-transfected for another 36 h as we described previously [21]. The efficiency of OGG1 depletion was determined at the protein level by Western blotting.

Statistical analyses

Values are presented as means \pm SEM. Statistical comparisons of differences were performed using one-way ANOVA combined with *t*-tests; $P < 0.05$ was considered statistically significant by Origin 9.

Results

OGG1-BER-associated increases in level of GTP-bound Rho in cultured cells and mouse lungs

To test for a link between repair of oxidative DNA damage and the activation of Rho-GTPases, cells were exposed to GOx, which has been reported to increase intracellular ROS levels and oxidative DNA damage [29]. Cell extracts were made and Rho-GTP levels were determined by active Rho pull-down assays. Our results showed that Rho-GTP levels had bipartite peaks, at 5 min and then at 30 min, in both MRC5 and MEF cells after exposure to GOx (Fig. 1A and B, respectively). To examine whether OGG1-BER has a role in Rho activation OGG1 expression was downregulated by followed by GOx exposure. Intriguingly, compared to control we observed no increase in Rho-GTP levels in extracts made from OGG1 depleted cells (Fig. 1C) suggesting an important role of OGG1-initiated BER and/or OGG1 in oxidative stress-induced Rho activation.

To examine the impact of OGG1-initiated repair of oxidative DNA damage and rule out multiple effects of ROS, we challenged cells with 8-oxoG base. Challenging MRC5 and MEF cells with 8-oxoG resulted in activation of Rho GTPase (between 2.5 and 20 min; Fig. 1D,E), suggesting that 8-oxoG challenge mimics OGG1-initiated repair of oxidatively damaged DNA. OGG1 excises 8-oxoG and 2,6-diamino-4-hydroxy-5-formamidopyrimidine (FapyG) from DNA with equal specificity and kinetics [3, 4]. Therefore, we challenged cells with FapyG. As shown in Fig. 1F, FapyG failed to increase GTP-bound levels of Rho, while positive 8-oxoG and calpeptin (a Rho activator) did so. Similarly, 8-oxo-deoxyguanosine (8-oxodG) failed to activate Rho GTPase in line with its inability to activate Ras and Rac family GTPases [19, 21]. To determine the percentage of Rho-GTP, autoradiograms were quantified using ImageJ software. In mock-exposed cells the calculated percentage of activated Rho was 1.06 and 1.45% (in MRC5 and MEF, respectively) upon 8-oxoG treatment, its level were between 3.8 and 8.3 % in MRC5 cells (Fig. 1D, lower panel), and 2.8 and 6.2 % in MEF cells (Fig 1E lower panel). Importantly, 8-oxoG-induced increase in Rho-GTP levels are similar to these mediated by oxidative stress (GOx)

(Fig. 1A,B, lower panels).

To further examine the role of OGG1 in 8-oxoG-mediated Rho activation, cells were depleted in OGG1 by siRNA and then challenged with 8-oxoG. Our results showed that a >80% OGG1 depletion (Fig. 1G, inset) nearly prevented 8-oxoG exposure-induced Rho activation in MRC5 cells (Fig. 1G). In support, 8-oxoG challenge rapidly increased Rho-GTP level in *Ogg1*^{+/+}, but not in *Ogg1*^{-/-} MEF cells (Fig. 1H).

To test whether Rho is activated in an organ/tissue environment as a consequence of OGG1-initiated BER, we challenged mice with 8-oxoG for 30 min and active Rho pull-down assays were undertaken. Results in Fig. 1I show increased levels of Rho-GTP in individual mouse lungs. Due to limitations in keeping time course, we generated extracts from unchallenged lungs and then added 8-oxoG. Our results showed that adding 8-oxoG base to lung extracts induced a rapid increase in GTP-bound Rho levels (Fig. 1J). The percentage changes in Rho-GTP in 8-oxoG treated lung extracts (Fig. 1J, lower panel) were similar to those observed in cell culture (Fig. 1 A,B and D,E), suggesting that in the presence of 8-oxoG base OGG1 in the extracts activates Rho.

Expression levels of RhoA, RhoB and RhoC vary significantly depending on cell/tissue type [30]. Utilizing isotype-specific antibodies (Abs), we observed that in both MRC5 and MEF cells, RhoA is the most abundant among the three family members (Fig. 1K), strongly suggesting that the observed increase in Rho-GTP levels is primarily represented by RhoA. Together, these data suggest that Rho activation requires OGG1 when cells exposed to oxidative stress or 8-oxoG a product of OGG1-initiated BER.

Interaction of OGG1 with RhoA and GDP→GTP exchange

Rho GTPases are inactive when GDP-bound and active when GTP-bound. Cycling between these states is controlled by three known classes of regulatory proteins: GTPase-activating proteins, guanine nucleotide dissociation inhibitors, and

GEFs [31]. The rapid OGG1-dependent increase in Rho-GTP levels upon ROS or 8-oxoG exposure suggests that OGG1 promotes GDP→GTP exchange, and may function as a GEF. To examine this possibility we first tested interactions between OGG1 and RhoA proteins. The results showed that the OGG1 protein physically interacts with RhoA (Fig. 2A). Addition of 8-oxoG base did not further increase OGG1 binding to RhoA (Fig. 2A). Furthermore, loading of RhoA with GTP or GDP had no effect on OGG1 ±8-oxoG binding to RhoA (Fig. 2B).

To test whether such binding could contribute to Rho activation, we examined the GDP→GTP exchange as previously described [21]. ^{Mant}GDP's fluorescence intensity is 1.33×10^5 fluorescence units (FU). When bound to RhoA, the fluorescence intensity was increased to 1.9×10^5 FU. Upon addition of OGG1 plus 8-oxoG along with unlabeled GTP, the fluorescence intensity of RhoA-^{Mant}GDP rapidly decreased, indicating that the RhoA-bound ^{Mant}GDP was replaced by non-fluorescent GTP. Fifty percentage of ^{Mant}GDP was replaced by GTP within 60 sec. In controls without the 8-oxoG base, OGG1 plus GTP did not change RhoA-^{Mant}GDP fluorescence. Neither did 8-oxoG base plus GTP, without OGG1 (Fig. 2C).

Next, we examined whether OGG1 catalyzes GTP→GDP exchange. Similar to ^{Mant}GDP, the fluorescence intensity of ^{Mant}GTP was increased (from 1.33×10^5 FU to 1.9×10^5 FU) when bound to RhoA. Upon addition of OGG1 plus 8-oxoG along with non-labeled GDP, there was no change in RhoA-^{Mant}GTP fluorescence intensity, implying the absence of any guanine nucleotide exchange. OGG1 or 8-oxoG alone caused no change in RhoA-^{Mant}GTP fluorescence in the presence of GDP (Fig. 2D). Together, these data suggest that OGG1 in complex with 8-oxoG function as a guanine nucleotide exchange factor.

OGG1-BER-associated α -SMA polymerization into stress fiber

To explore the functional consequence of OGG1-BER-mediated activation of RhoA in a cellular context, changes in stress fiber levels were examined. To do so, we utilized serum-starved MRC5 and MEF cells to visualize cytoskeletal changes

microscopically by using FITC-phalloidin. Microscopic imaging showed that in mock-treated cells the bound level of FITC-phalloidin was low. Importantly, exposure of cells to 8-oxoG induced obvious changes in the cytoskeleton, as shown by the appearance of stress fibers in both MRC5 and MEF cells (Fig. 3A). Furthermore, these changes were not observed in OGG1-knock-out cells (Fig. 3A, lowest panel), in line with the dependence on OGG1 in the 8-oxoG-induced increases in Rho-GTP levels (shown in Fig. 1I). As a positive control, the Rho activator calpeptin (1 unit/ml) induced formation of stress fiber in MRC5 cells and MEF (both OGG1^{+/+} and OGG1^{-/-} ones). In addition to MRC5 and MEF cells, human normal bronchial epithelial cells (hNBECs) were also affected by 8-oxoG exposure displaying stress fibers (Fig. 3B). This implies that not only fibroblasts, but also epithelial cells respond to 8-oxoG and possibly to OGG1-initiated repair of oxidative DNA damage with cytoskeletal changes.

Stress fibers that contain α -SMA generate more contractile force than do stress fibers that contain only β - and γ -cytoplasmic actin [32]. To test whether α -SMA level was increased in the fibers, MRC-5 and MEF cells were exposed to 8-oxoG and analyzed by Western blotting. Our results showed that from 10 min on, the level of α -SMA was increased in stress fibers in MRC-5 and MEF cells (Fig. 3C-D), suggesting that α -SMA is incorporated into stress fibers in response to 8-oxoG exposure. In contrast, there was no obvious increase in α -SMA levels in the stress fibers of *Ogg1*^{-/-} MEFs in response to 8-oxoG (Fig. 3E). These results support the idea that OGG1-dependent Rho activation is the primary reason for α -SMA polymerization into stress fibers upon 8-oxoG addition.

To further explore the importance of OGG1 in activation of Rho and α -SMA polymerization, OGG1 was depleted from MRC5 cells via siRNA. Cells with decreased (~80%) OGG1 showed no obvious increase in α -SMA in stress fibers after exposure to 8-oxoG (Fig. 3F). To test whether Rho activation is the primary cause of stress fiber formation by 8-oxoG exposure, we utilized a Rho inhibitor (C3 transferase, 2 μ g/ml), shown previously to prevent formation of stress fibers [33]. Pre-incubation of cells with C3 transferase significantly decreased the level of α -SMA in the stress

fibers in *Ogg1*^{+/+} MEF cells (Fig. 3G). These data strongly suggest that 8-oxoG exposure-induced α -SMA incorporation into stress fibers is OGG1-dependent, linking OGG1-initiated repair of oxidative DNA damage to cellular cytoskeletal changes.

Cytoskeletal changes in mouse lungs upon 8-oxoG challenge

Next we examined whether the cytoskeleton was changed in mouse lungs after 8-oxoG challenge. The lungs were challenged intranasally with 8-oxoG to increase then excised and sectioned (see Materials and Methods). Microscopic imaging showed an increased co-localization of α -SMA with F-actin in subepithelial regions of lung bronchioles (Fig. 4A), suggesting that α -SMA is polymerized into the cytoskeleton in response to 8-oxoG. To confirm the incorporation of soluble α -SMA into stress fibers, lungs were homogenized and the Triton X-100-insoluble fractions isolated and subjected to immunoblotting. As shown in Fig. 4B, 8-oxoG-challenge increased α -SMA levels in the Triton X-100-insoluble cytoskeletal fractions of mouse lungs.

Moreover, this increase was accompanied by a decrease in α -SMA levels in the soluble fraction. To validate the method used for this *in vivo* observation, MRC-5 cells were exposed to 8-oxoG and fractionated into Triton X-100-insoluble/soluble fractions similarly as for lung tissue. Immunoblotting showed α -SMA redistribution into insoluble fraction in response to 8-oxoG (Fig. 4C). These results imply that α -SMA is incorporated into Triton X-100-insoluble cytoskeletal fraction in response to 8-oxoG both in lungs and in cultured cells.

Discussion

Supraphysiological levels of 8-oxoG in the genome has been linked to various diseases, including malignancies, aging-related neurological diseases and aging processes themselves [34-38]. A common link among these processes is change(s) in actin cytoskeleton, cell-cell interactions, and extracellular matrix and nearly all thought to be etiologically linked to oxidative stress [39]. Here we show that only OGG1-expressing cells showed increased Rho activation and α -SMA polymerization into stress fibers in response to oxidative stress exposure of cells. Thus our data provide the first evidence for an association between OGG1-initiated repair of oxidative DNA damage and changes in cytoskeleton, which may be one among multiple mechanistic explanations for the link between OGG1-BER and aging as well as the development of diseases.

Our present study shows an OGG1 expression-dependent increase in Rho-GTP level upon oxidative stress exposure. Increases in Rho-GTP levels were biphasic, therefore we speculated that the immediate early peak could be due to ROS since Rho has a redox-sensitive motif containing two cysteine residues (GXXXCGK{S/T}C) in the phosphate-binding loop [40, 41], while the second peak may be a result of OGG1 BER. To pursue the later hypothesis we challenged cells with 8-oxoG, which increased levels of Rho-GTP only in OGG1-expressing cells implying that both OGG1 and 8-oxoG base one of the product of OGG1-BER is important to Rho activation.

In theory, activation of Rho GTPases could occur through stimulation of a GEF or inhibition of GTPase activating factor (GAP); in practice, however, all evidence points to GEFs being the most critical mediators of Rho GTPase activation [42]; these have the ability to catalyze the exchange of GDP→GTP on Rho GTPases. Such actions of GEFs can be measured by their ability to stimulate nucleotide exchange *in vitro* [21]. To obtain initial information on the role of its GEF activity, we first examined OGG1's ability to bind RhoA *in vitro*. The OGG1 protein physically interacts with Rho protein. Interestingly, interactions between OGG1 and Rho did not require 8-oxoG base *in vitro*, which is different from the binding of OGG1 to Ras or

Rac1 [19, 21]. At this time, we have no information on *in cellulo* interactions between OGG1 and RhoA; however, the rapid activation of Rho upon OGG1-initiated BER, mimicked by the addition of the OGG1-BER product 8-oxoG base strongly suggests their interaction. Furthermore, in the presence of 8-oxoG base, OGG1 efficiently catalyzed exchange of Rho-^{Mant}GDP with GTP. These results were not entirely surprising, as OGG1 plus 8-oxoG functions as a guanine nucleotide release factor for canonical Ras family GTPases [19], while it has GEF activity for Rac1, as we showed previously [21]. In our experiments, substitution of ^{Mant}GTP for unlabeled GTP was not detectable, suggesting that OGG1 primarily catalyzes GDP→GTP exchange. These data are consistent with those showing that during guanine nucleotide exchange, GEFs interact with GDP-bound GTPases and dissociate GDP at an increased rate, and the bound GTP then promotes the release of the GEF from the GTPase [43, 44].

GEFs require post-translational modifications to activate Rho GTPases [45, 46]. In the case of OGG1, its repair product 8-oxoG base was required for GDP→GTP exchange. Indeed, a previous study showed that OGG1 binds the free 8-oxoG base with high affinity (binding constant $\{K_d\}$ 0.56±0.19 nM) [19]). OGG1's binding by 8-oxoG was found to be necessary for activation of Ras and Rac1. It was thus unexpected that OGG1's binding by 8-oxoG is not necessary for interaction with Rho, but it was essential for Rho guanine nucleotide exchange. These results allow us to speculate that Rho-associated OGG1 binds 8-oxoG, and then mediates GDP→GTP exchange. It has been shown that OGG1 not only excises 8-oxoG, but also FapyG from DNA with equal specificity and kinetics [4]. In view of these facts, we wondered if FapyG exposure of cells increased Rho-GTP levels. Results were negative. Lack of Rho activation by FapyG is consistent with data showing its undetectable binding to OGG1, which was previously analyzed by changes in OGG1's intrinsic tryptophan (Trp) fluorescence [19].

Conventionally, Rho activation modulates the assembly of contractile actomyosin stress fibers, Rac-GTP produces lamellipodia and membrane ruffles, and Cdc42 induces filopodia formation [30]. To gain insight into the possible biological consequences of OGG1-BER-associated Rho activation, we examined changes in the

α -SMA polymerization into stress fibers, a process primarily driven by RhoA-GTP. Our data show that activation of Rho due to OGG1-BER mimicked by the addition of 8-oxoG base resulted in increased stress fiber content in both MRC5 and MEF fibroblasts, as shown first using microscopic imaging. To build upon the imaging data, we showed an OGG1-dependent increase in levels of α -SMA in the insoluble cellular fractions.

ROS-induced signaling pathways are involved in distinct cellular biological processes, such as proliferation, cell-cell interactions, cell migration, (re)-organization of intracellular filaments, and regulation of the extracellular matrix [39]. There is evidence that suitably activated fibroblasts can give rise to a differentiated phenotype characterized by the induction of α -SMA, which is incorporated into stress fibers, so the cells are aptly identified as myofibroblasts [47]. In our studies we primarily utilized fibroblast cells and carried out *in vivo* experiments, and demonstrated that ROS-induced DNA damage/repair-driven Rho activation converts fibroblasts to α -SMA-positive cells, which is one of the myofibroblast phenotypes. To circumvent implication of ROS in Rho activation and α -SMA polymerization into stress fibers, most of our studies utilized a specific product of OGG1-initiated BER, 8-oxoG base. Our results showing that 8-oxoG base exposure of cells leads to increased Rho-GTP levels raise the possibility that OGG1-BER is coupled to cellular morphological changes and the regulation of the cytoskeleton via Rho in oxidatively stressed cells. To test whether OGG1-BER and release of 8-oxoG are key events in Rho activation and changes in cytoskeleton, OGG1-initiated BER was prevented using siRNA specific for OGG1. As expected, ablation of OGG1 significantly decreased Rho activation both in oxidatively stressed and 8-oxoG-challenged cells.

In our studies, we utilized experimental animals to show the translational significance of our studies. Our rationale for using the lungs was that they directly interact with the environment and are exposed to pollutants resulting in oxidative stress, and consequently DNA damage [48], including guanine oxidation, that is subject to repair via OGG1-BER. In addition, major age- and occupation-related chronic airway diseases (e.g., asthma and COPD) are associated with tissue

remodeling, which thought to be related to an increased oxidative state and DNA damage [49]. In 8-oxoG base challenged mouse lungs RhoA was activated consequently α -SMA is polymerized into the cytoskeleton and accumulated in insoluble fractions. Thus our data may give us a clue to a mechanism by which ROS-induced DNA damage and OGG1-initiated repair of oxidative DNA damage play roles in lung remodeling, and fibrosis, including idiopathic pulmonary fibrosis. These cellular pathological changes are usually linked to decreased DNA repair, including OGG1-BER. Interestingly, our findings show the opposite, the involvement of OGG1-initiated BER in cytoskeletal changes. One may propose that oxidative stress, generation of DNA base damage and the consequent DNA repair by OGG1 could be involved in organ/tissue remodeling observed in various chronic diseases or aging-associated processes. Although it should be proven experimentally, we speculate that decreased OGG1 activity observed in fibrotic tissues and malignant cells, for example, could be a cellular defense against extensive cellular cytoskeletal changes that are required for the proliferation and migration of cancerous cells.

Conflict of interest statement

There are no conflicts of interest.

Acknowledgements

This work was supported by grants NIEHS RO1 ES018948 (IB), NIA/AG 021830 (IB) NIAID/AI062885 (IB), and the NHLBI Proteomic Center, N01HV00245 (Dr. A. Kurosky); International Science-Technology Collaboration Foundation (20120728) of Jilin Province in China (XB), TAMOP 4.2.1/B-09/1/KONV-2010-2007 project, which is co-financed by the European Union and the European Social Fund. AB was also supported by the Janos Bolyai Fellowship from the Hungarian Academy of Sciences. We thank Dr. David Konkel (Institute for Translational Sciences, UTMB) and Mardelle Susman (Microbiology and Immunology, UTMB) for their scientific input and critically editing of the manuscript.

Figure Legends

Figure 1 Activation of Rho-GTPase coincides with OGG1-initiated BER. (A-B) Increased Rho-GTP levels in cultured cells exposed to oxidative stress. MRC-5 (A) and MEF (B) cells were exposed to GOx (100 ng/ml) and lysed at the times indicated. Rho-GTP levels were determined in 500 µg cell extracts by Active Rho pull-down assays. (C) OGG1 depletion decreased Rho activation. MRC5 cells were transfected with siRNA to OGG1 or control siRNA and exposed to GO for 5 min. Rho-GTP was determined as in legend to A-B. (D,E) The OGG1-BER product 8-oxoG base increases Rho-GTP levels. MRC5 (D) and MEF (E) cells were exposed to 8-oxoG (10 µM) at 37 °C, cell extracts prepared at the indicated times, and Rho-GTP levels determined as in A-B. (F) Lack of Rho activation in FapyG-exposed cells. Cells were exposed to FapyG (10 µM) and cell extracts were prepared at 5 min and Rho-GTP levels determined as in A-B. As controls, calpeptin (a Rho activator) and 8-oxodG were used. (G) OGG1 depletion prevents Rho activation in 8-oxoG-exposed cells. MRC5 cells were transfected with OGG1 or control siRNA and exposed to 8-oxoG for 5 min. Rho-GTP was determined as in legend to A-B. Inset, extent of OGG1 downregulation by siRNA. (H) Lack of 8-oxoG-induced Rho activation in *Ogg1*^{-/-} MEFs. Cells (*Ogg1*^{-/-} and *Ogg1*^{+/+}) were challenged with 8-oxoG, extracts were made at 5 min, and changes in Rho-GTP levels determined by pull-down assays as in legend to A-B. (I) Activation of Rho GTPase in mouse lungs. Mice were challenged with 8-oxoG (1 µM) via intranasal route and at 30 min active Rho was determined by pull-down assays. (J) Activation of Rho in lung extracts by 8-oxoG. Lung extracts from unchallenged mice were incubated with 10 µM 8-oxoG as indicated and changes in Rho-GTP levels determined as in A and B. Lower panels to A, B, D, E and J show graphical depiction of the % of activated Rho. Band intensities were analyzed with Image J software and the percentage of active Rho in total Rho was calculated. (K) Expression of Rho isoforms in MRC-5, *Ogg1*^{-/-} and *Ogg1*^{+/+} MEF cells. Cell extracts (20 µg) were subjected to SDS-PAGE and RhoA, B, C levels were determined by immunoblotting using type-specific Abs. GAPDH levels show equal loading. Cont =

control. MEF, mouse embryonic fibroblast cells, MRC5, human embryonic lung fibroblast cells. Each experiment was repeated at least 3 times. * $p < 0.05$, ** $p < 0.01$

Figure 2 Interaction of OGG1 with RhoA protein and guanine nucleotide exchange in the presence of 8-oxoG base. (A) Physical interaction of OGG1 protein with RhoA. His-RhoA (6 pmol) bound to Ni-NTA was incubated with OGG1 protein (6 pmol) for 30 min \pm 8-oxoG (6 pmol). OGG1 binding to Rho was detected by Western Blot analysis. (B) Physical interaction of OGG1 protein with RhoA in the presence of GDP, GTP and/or 8-oxoG was detected as described in A. (C) Exchange of RhoA-bound GDP to GTP by OGG1 in the presence of the 8-oxoG base. RhoA protein (6 pmol) was loaded with ^{Mant}GDP (6 pmol) and nucleotide exchange was initiated by adding OGG1+8-oxoG and GTP (6 pmol) (■). In controls, RhoA-^{Mant}GDP+GTP+OGG1 (▲), RhoA-^{Mant}GDP + GTP+ 8-oxoG (◆) or ^{Mant}GDP+GTP+OGG1+8-oxoG (×) did not catalyze RhoA-GTP→GDP exchange. (D) OGG1 does not catalyze RhoA-GTP→GDP exchange. RhoA loaded with ^{Mant}GTP was incubated with GDP+OGG1+8-oxoG (■), GDP+8-oxoG (◆), or GDP+OGG1 (▲). ^{Mant}GTP alone (●). In C and D, changes in the fluorescence of RhoA-^{Mant}GDP and RhoA-^{Mant}GTP were determined by real-time measurements using a POLARstar Omega (BMG LABTECH Germany). Curves were fitted using MS Excel, $n=3-5$.

Figure 3 α -SMA polymerization into stress fibers in OGG1-expressing cells. (A) MRC5 and MEF cells and (B) hNBECs were challenged with 8-oxoG (10 μ M) for 20 min, fixed and stained with FITC-phalloidin. Representative images were taken using a NIKON Eclipse Ti microscope system ($\times 192$ magnification). As a positive control, cells were incubated with the Rho activator calpeptin (1 unit/ml) for 20 min. (C-E) Cells were treated with 8-oxoG (10 μ M) for the indicated times and insoluble fractions were isolated as described in Materials and Methods. α -SMA polymerized into stress fibers was detected by Western Blot analysis. (F) MRC5 cells were transfected with OGG1-specific or control siRNA as described in Materials and Methods, and α -SMA in stress fibers examined 20 min after challenge with 8-oxoG.

(G) MRC5 cells were incubated with the Rho inhibitor C3 transferase (2 $\mu\text{g}/\text{ml}$) for 4 h before a 20 min 8-oxoG challenge. Insoluble fractions were isolated and α -SMA in the isolated fractions analyzed by Western blotting. SF, stress fiber, SF- α -SMA, α -SMA in the stress fibers; Cont = control; hNBECs, human normal bronchial epithelial cells; FITC, fluorescein isothiocyanate. Each experiment was repeated at least 3 times.

Figure 4 8-oxoG base-induced α -SMA polymerization in lungs. (A) Lungs were 8-oxoG (1 μM)-challenged and excised 30 min thereafter, fixed, sectioned and stained with antibody to α -SMA (red) and F-actin (green). Images were taken using a NIKON Eclipse Ti microscope system ($\times 138$ magnification). (B) Lungs were excised and the trachea and bronchial branches removed and homogenized in cytoskeleton lysis buffer. Triton X-100-insoluble (cytoskeletal) and soluble fractions were subjected to PAGE. α -SMA (and α -tubulin and GAPDH used as loading controls) was detected using specific antibodies. (C) MRC5 cells were exposed to 8-oxoG (10 μM) for 20 min and Triton X-100-insoluble and soluble fractions were analyzed as in the legend to B. Cont = control. Each experiment was repeated at least 3 times.

References

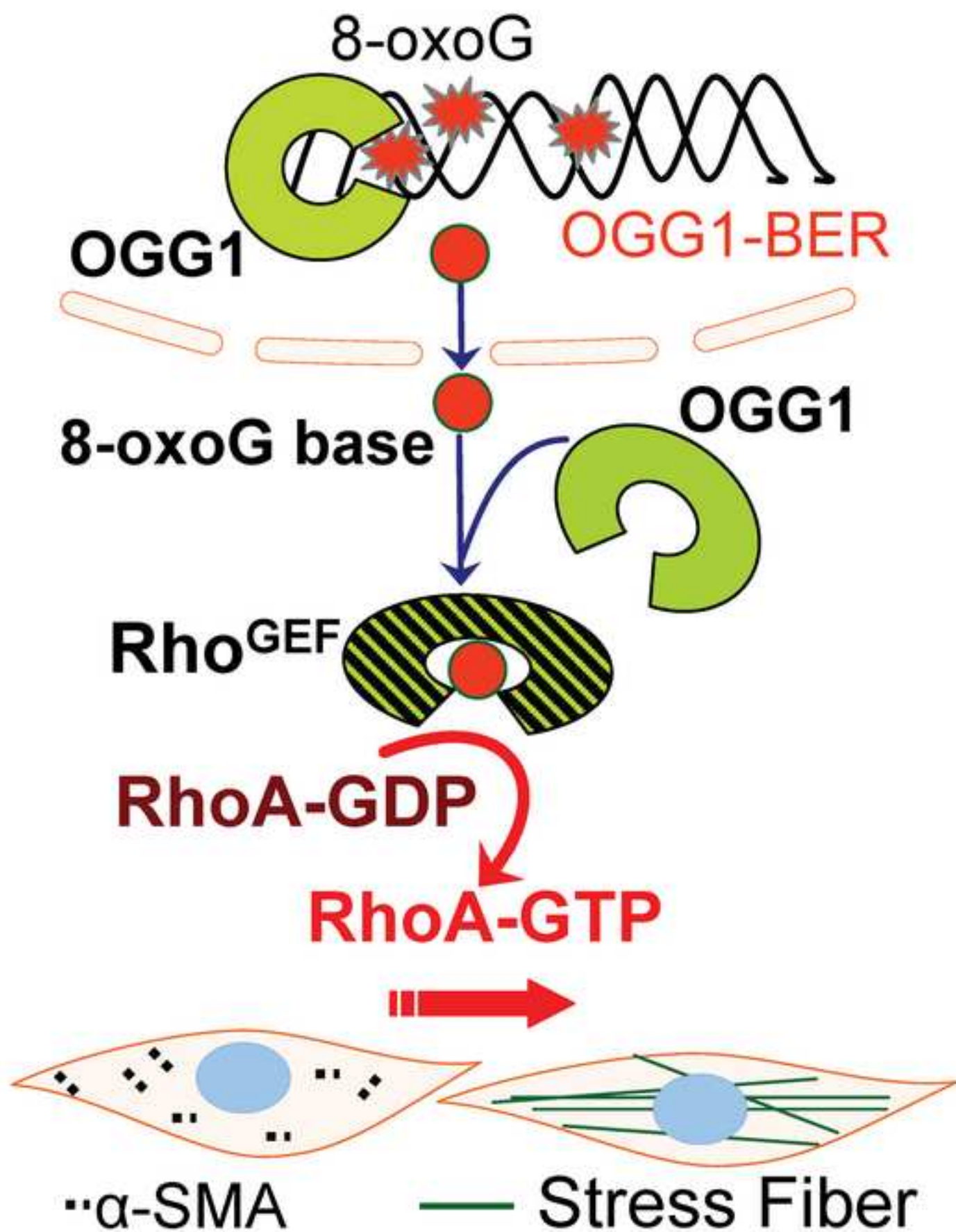
- [1] Loft, S.; Hogh Danielsen, P.; Mikkelsen, L.; Risom, L.; Forchhammer, L.; Moller, P. Biomarkers of oxidative damage to DNA and repair. *Biochem Soc Trans* **36**:1071-1076; 2008.
- [2] Margolin, Y.; Cloutier, J. F.; Shafirovich, V.; Geacintov, N. E.; Dedon, P. C. Paradoxical hotspots for guanine oxidation by a chemical mediator of inflammation. *Nat Chem Biol* **2**:365-366; 2006.
- [3] Dizdaroglu, M.; Kirkali, G.; Jaruga, P. Formamidopyrimidines in DNA: mechanisms of formation, repair, and biological effects. *Free Radic Biol Med* **45**:1610-1621; 2008.
- [4] Cooke, M. S.; Evans, M. D.; Dizdaroglu, M.; Lunec, J. Oxidative DNA damage: mechanisms, mutation, and disease. *Faseb J* **17**:1195-1214; 2003.
- [5] Radak, Z.; Boldogh, I. 8-Oxo-7,8-dihydroguanine: links to gene expression, aging, and defense against oxidative stress. *Free Radic Biol Med* **49**:587-596; 2010.
- [6] Mitra, S.; Izumi, T.; Boldogh, I.; Bhakat, K. K.; Hill, J. W.; Hazra, T. K. Choreography of oxidative damage repair in mammalian genomes. *Free Radic Biol Med* **33**:15-28; 2002.
- [7] David, S. S.; O'Shea, V. L.; Kundu, S. Base-excision repair of oxidative DNA damage. *Nature* **447**:941-950; 2007.
- [8] Rosenquist, T. A.; Zharkov, D. O.; Grollman, A. P. Cloning and characterization of a mammalian 8-oxoguanine DNA glycosylase. *Proc Natl Acad Sci U S A* **94**:7429-7434; 1997.
- [9] Nishimura, S. Involvement of mammalian OGG1(MMH) in excision of the 8-hydroxyguanine residue in DNA. *Free Radic Biol Med* **32**:813-821; 2002.
- [10] Sassa, A.; Beard, W. A.; Prasad, R.; Wilson, S. H. DNA sequence context effects on the glycosylase activity of human 8-oxoguanine DNA glycosylase. *J Biol Chem* **287**:36702-36710; 2012.
- [11] Klungland, A.; Rosewell, I.; Hollenbach, S.; Larsen, E.; Daly, G.; Epe, B.; Seeberg, E.; Lindahl, T.; Barnes, D. E. Accumulation of premutagenic DNA lesions

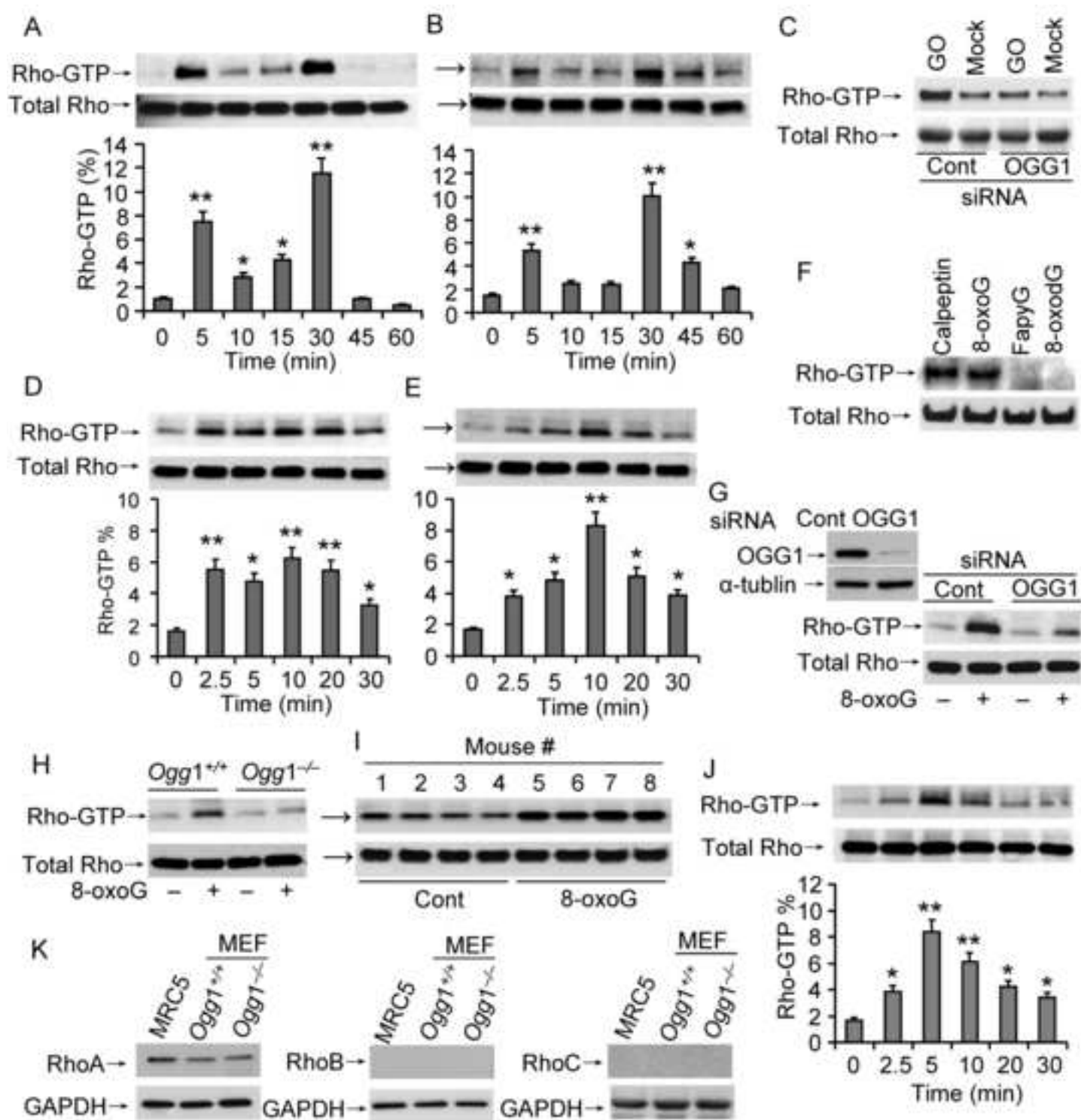
- in mice defective in removal of oxidative base damage. *Proc Natl Acad Sci U S A* **96**:13300-13305; 1999.
- [12] Sakumi, K.; Tominaga, Y.; Furuichi, M.; Xu, P.; Tsuzuki, T.; Sekiguchi, M.; Nakabeppu, Y. Ogg1 knockout-associated lung tumorigenesis and its suppression by Mth1 gene disruption. *Cancer Res* **63**:902-905; 2003.
- [13] Minowa, O.; Arai, T.; Hirano, M.; Monden, Y.; Nakai, S.; Fukuda, M.; Itoh, M.; Takano, H.; Hippou, Y.; Aburatani, H.; Masumura, K.; Nohmi, T.; Nishimura, S.; Noda, T. Mmh/Ogg1 gene inactivation results in accumulation of 8-hydroxyguanine in mice. *Proc Natl Acad Sci U S A* **97**:4156-4161; 2000.
- [14] Mabley, J. G.; Pacher, P.; Deb, A.; Wallace, R.; Elder, R. H.; Szabo, C. Potential role for 8-oxoguanine DNA glycosylase in regulating inflammation. *FASEB J* **19**:290-292; 2005.
- [15] Sampath, H.; Vartanian, V.; Rollins, M. R.; Sakumi, K.; Nakabeppu, Y.; Lloyd, R. S. 8-Oxoguanine DNA glycosylase (OGG1) deficiency increases susceptibility to obesity and metabolic dysfunction. *PLoS One* **7**:e51697; 2012.
- [16] Conlon, K. A.; Zharkov, D. O.; Berrios, M. Cell cycle regulation of the murine 8-oxoguanine DNA glycosylase (mOGG1): mOGG1 associates with microtubules during interphase and mitosis. *DNA Repair (Amst)* **3**:1601-1615; 2004.
- [17] Dantzer, F.; Luna, L.; Bjoras, M.; Seeberg, E. Human OGG1 undergoes serine phosphorylation and associates with the nuclear matrix and mitotic chromatin in vivo. *Nucleic Acids Res* **30**:2349-2357; 2002.
- [18] Fromme, J. C.; Bruner, S. D.; Yang, W.; Karplus, M.; Verdine, G. L. Product-assisted catalysis in base-excision DNA repair. *Nat Struct Biol* **10**:204-211; 2003.
- [19] Boldogh, I.; Hajas, G.; Aguilera-Aguirre, L.; Hegde, M. L.; Radak, Z.; Bacsi, A.; Sur, S.; Hazra, T. K.; Mitra, S. Activation of ras signaling pathway by 8-oxoguanine DNA glycosylase bound to its excision product, 8-oxoguanine. *J Biol Chem* **287**:20769-20773; 2012.
- [20] German, P.; Szaniszló, P.; Hajas, G.; Radak, Z.; Bacsi, A.; Hazra, T. K.; Hegde, M. L.; Ba, X.; Boldogh, I. Activation of cellular signaling by 8-oxoguanine DNA

- glycosylase-1-initiated DNA base excision repair. *DNA Repair (Amst)* **12**:856-863; 2013.
- [21] Hajas, G.; Bacsı, A.; Aguilera-Aguirre, L.; Hegde, M. L.; Tapas, K. H.; Sur, S.; Radak, Z.; Ba, X.; Boldogh, I. 8-Oxoguanine DNA glycosylase-1 links DNA repair to cellular signaling via the activation of the small GTPase Rac1. *Free Radic Biol Med* **61C**:384-394; 2013.
- [22] Soza, S.; Leva, V.; Vago, R.; Ferrari, G.; Mazzini, G.; Biamonti, G.; Montecucco, A. DNA ligase I deficiency leads to replication-dependent DNA damage and impacts cell morphology without blocking cell cycle progression. *Mol Cell Biol* **29**:2032-2041; 2009.
- [23] Giry, M.; Popoff, M. R.; von Eichel-Streiber, C.; Boquet, P. Transient expression of RhoA, -B, and -C GTPases in HeLa cells potentiates resistance to *Clostridium difficile* toxins A and B but not to *Clostridium sordellii* lethal toxin. *Infect Immun* **63**:4063-4071; 1995.
- [24] Boldogh, I.; Bacsı, A.; Choudhury, B. K.; Dharajiya, N.; Alam, R.; Hazra, T. K.; Mitra, S.; Goldblum, R. M.; Sur, S. ROS generated by pollen NADPH oxidase provide a signal that augments antigen-induced allergic airway inflammation. *J Clin Invest* **115**:2169-2179; 2005.
- [25] Reid, T.; Furuyashiki, T.; Ishizaki, T.; Watanabe, G.; Watanabe, N.; Fujisawa, K.; Morii, N.; Madaule, P.; Narumiya, S. Rhotekin, a new putative target for Rho bearing homology to a serine/threonine kinase, PKN, and rhotekin in the rho-binding domain. *J Biol Chem* **271**:13556-13560; 1996.
- [26] Zhang, B.; Zhang, Y.; Wang, Z.; Zheng, Y. The role of Mg²⁺ cofactor in the guanine nucleotide exchange and GTP hydrolysis reactions of Rho family GTP-binding proteins. *J Biol Chem* **275**:25299-25307; 2000.
- [27] Liu, T.; Guevara, O. E.; Warburton, R. R.; Hill, N. S.; Gaestel, M.; Kayyali, U. S. Regulation of vimentin intermediate filaments in endothelial cells by hypoxia. *Am J Physiol Cell Physiol* **299**:C363-373; 2010.
- [28] Katoh, K.; Kano, Y.; Masuda, M.; Onishi, H.; Fujiwara, K. Isolation and contraction of the stress fiber. *Mol Biol Cell* **9**:1919-1938; 1998.

- [29] Das, S.; Chattopadhyay, R.; Bhakat, K. K.; Boldogh, I.; Kohno, K.; Prasad, R.; Wilson, S. H.; Hazra, T. K. Stimulation of NEIL2-mediated oxidized base excision repair via YB-1 interaction during oxidative stress. *J Biol Chem* **282**:28474-28484; 2007.
- [30] Wheeler, A. P.; Ridley, A. J. Why three Rho proteins? RhoA, RhoB, RhoC, and cell motility. *Exp Cell Res* **301**:43-49; 2004.
- [31] Rossman, K. L.; Der, C. J.; Sondek, J. GEF means go: turning on RHO GTPases with guanine nucleotide-exchange factors. *Nat Rev Mol Cell Biol* **6**:167-180; 2005.
- [32] Hinz, B.; Mastrangelo, D.; Iselin, C. E.; Chaponnier, C.; Gabbiani, G. Mechanical tension controls granulation tissue contractile activity and myofibroblast differentiation. *Am J Pathol* **159**:1009-1020; 2001.
- [33] Uehata, M.; Ishizaki, T.; Satoh, H.; Ono, T.; Kawahara, T.; Morishita, T.; Tamakawa, H.; Yamagami, K.; Inui, J.; Maekawa, M.; Narumiya, S. Calcium sensitization of smooth muscle mediated by a Rho-associated protein kinase in hypertension. *Nature* **389**:990-994; 1997.
- [34] Shao, C.; Xiong, S.; Li, G. M.; Gu, L.; Mao, G.; Markesbery, W. R.; Lovell, M. A. Altered 8-oxoguanine glycosylase in mild cognitive impairment and late-stage Alzheimer's disease brain. *Free Radic Biol Med* **45**:813-819; 2008.
- [35] Kaneko, T.; Tahara, S.; Matsuo, M. Non-linear accumulation of 8-hydroxy-2'-deoxyguanosine, a marker of oxidized DNA damage, during aging. *Mutat Res* **316**:277-285; 1996.
- [36] Markesbery, W. R.; Lovell, M. A. DNA oxidation in Alzheimer's disease. *Antioxid Redox Signal* **8**:2039-2045; 2006.
- [37] Wilson, D. M., 3rd; Bohr, V. A. The mechanics of base excision repair, and its relationship to aging and disease. *DNA Repair (Amst)* **6**:544-559; 2007.
- [38] Hegde, M. L.; Mantha, A. K.; Hazra, T. K.; Bhakat, K. K.; Mitra, S.; Szczesny, B. Oxidative genome damage and its repair: implications in aging and neurodegenerative diseases. *Mech Ageing Dev* **133**:157-168; 2012.
- [39] Gourlay, C. W.; Ayscough, K. R. The actin cytoskeleton: a key regulator of apoptosis and ageing? *Nat Rev Mol Cell Biol* **6**:583-589; 2005.

- [40] Heo, J.; Raines, K. W.; Mocanu, V.; Campbell, S. L. Redox regulation of RhoA. *Biochemistry* **45**:14481-14489; 2006.
- [41] Aghajanian, A.; Wittchen, E. S.; Campbell, S. L.; Burrige, K. Direct activation of RhoA by reactive oxygen species requires a redox-sensitive motif. *PLoS One* **4**:e8045; 2009.
- [42] Van Aelst, L.; D'Souza-Schorey, C. Rho GTPases and signaling networks. *Genes Dev* **11**:2295-2322; 1997.
- [43] Bourne, H. R.; Sanders, D. A.; McCormick, F. The GTPase superfamily: a conserved switch for diverse cell functions. *Nature* **348**:125-132; 1990.
- [44] Boriack-Sjodin, P. A.; Margarit, S. M.; Bar-Sagi, D.; Kuriyan, J. The structural basis of the activation of Ras by Sos. *Nature* **394**:337-343; 1998.
- [45] Bickle, M.; Delley, P. A.; Schmidt, A.; Hall, M. N. Cell wall integrity modulates RHO1 activity via the exchange factor ROM2. *Embo J* **17**:2235-2245; 1998.
- [46] Schmidt, A.; Hall, A. Guanine nucleotide exchange factors for Rho GTPases: turning on the switch. *Genes Dev* **16**:1587-1609; 2002.
- [47] Kis, K.; Liu, X.; Hagood, J. S. Myofibroblast differentiation and survival in fibrotic disease. *Expert Rev Mol Med* **13**:e27; 2011.
- [48] Kinnula, V. L.; Crapo, J. D. Superoxide dismutases in the lung and human lung diseases. *Am J Respir Crit Care Med* **167**:1600-1619; 2003.
- [49] Faner, R.; Rojas, M.; Macnee, W.; Agusti, A. Abnormal lung aging in chronic obstructive pulmonary disease and idiopathic pulmonary fibrosis. *Am J Respir Crit Care Med* **186**:306-313; 2012.





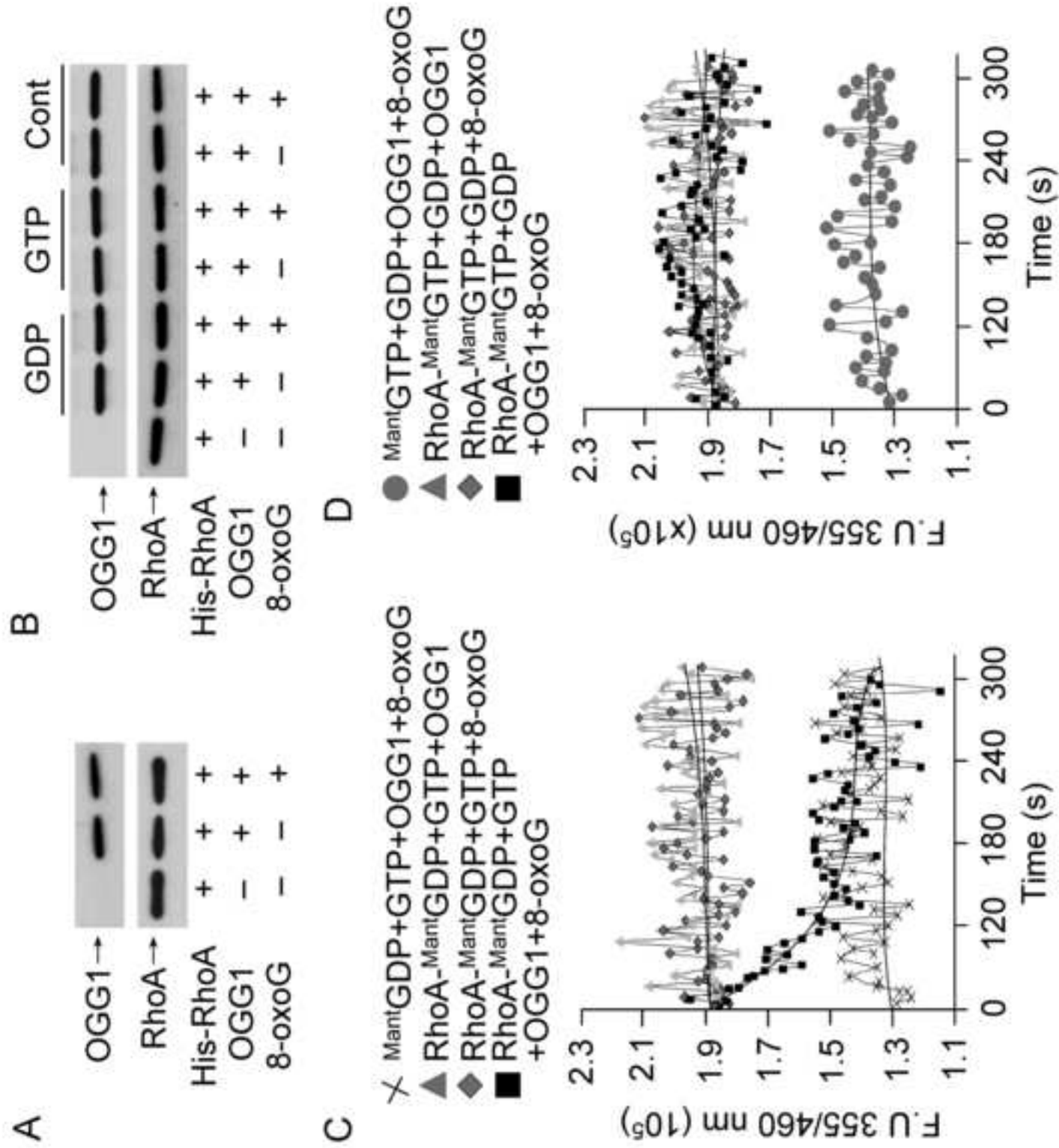


Figure 2

